Electric Thermal Storage System Impact on Northern Communities' Microgrids

Patrick S. Sauter, *Student Member, IEEE,* Bharatkumar V. Solanki, *Student Member, IEEE,*
Claudio A. Cañizares, *Fellow IEEE,* Kankar Bhattacharya, *Fellow IEEE,* and Sören Hohmann, *Member, IEEE*

***Abstract*—In this paper, the impact of Electric Thermal Storage (ETS) systems on the operation of Northern Communities' microgrids is analyzed. A mathematical model of the ETS system is developed and integrated into an Energy Management System (EMS) for isolated microgrids, in which the problem is divided into Unit Commitment (UC) and Optimal Power Flow (OPF) subproblems, to dispatch fossil-fuel-based generators, Energy Storage Systems (ESS), and ETS charging. To account for the deviations in the forecast of renewables, a Model Predictive Control (MPC) technique is used. The proposed ETS-EMS framework is tested and studied on a modified CIGRE medium voltage benchmark system, which comprises various kinds of Distributed Energy Resources (DER), and on the real Kasabonika Lake First Nation (KLFN) isolated microgrid system. It is shown that the ETS significantly reduces operating costs, and allows for better integration of intermittent wind and solar sources.**

***Index Terms*—Demand response, electric thermal storage, microgrid, Optimal Power Flow, renewable energy integration, Unit Commitment.**

NOMENCLATURE

Indices and Superscripts

g	Generating units
i, j	Bus
k	Time steps
n	ESS units
^{c}	Commercial
^{r}	Residential
^{EL}	Electric
TH	Thermal

Sets

$\mathcal{G}_i$	Generator units connected to bus *i*
$\mathcal{N}_i$	ESS units connected to bus *i*
$\mathcal{T}$	Time steps

Parameters

a	Quadratic term of cost function [\$/kWh^2]
b	Linear term of cost function [\$/kWh]
c	Constant term of cost function [\$/h]
C^{LC}	Load curtailment cost [\$/kWh]
C^L	Cost of ETS effective self-discharge [\$/kWh]
C^{sdn}	Shut-down cost of generating unit [\$]
C^{sup}	Start-up cost of generating unit [\$]
$\overline{PESS}$	ESS charging/discharging power limit [p.u.]
P^{TH}	Thermal demand served by electric heating [p.u.]
P_S^{TH}	Thermal discharge set point [p.u.]
PD	Active power demand [p.u.]
PV	Photo-Voltaic (PV) plant output [p.u.]
PW	Wind turbine output [p.u.]
QD	Reactive power demand [p.u.]
R^{dn}	Ramp-down rate of generating unit [p.u./h]
R^{up}	Ramp-up rate of generating unit [p.u./h]
T^{dn}	Minimum down-time of generating unit [h]
T^{up}	Minimum up-time of generating unit [h]
T_a	Ambient temperature [°C]
T_r	Room temperature [°C]
T_s	Temperature set point [°C]
x_i	Number of electric heating units at bus *i*
α	Voltage exponent for active load model
$\bar{}, \underline{}$	Maximum and minimum limits
β	Voltage exponent for reactive load model
Δt_k	Time interval between step k and step $k+1$ [h]
η^{ch}, η^{dch}	Charging, discharging efficiency of ESS
η_{ETS}	ETS electric-thermal energy conversion efficiency
η_S	Thermal storage efficiency of ETS
μ_i	% electric heating units replaced by ETS at bus *i*
$\hat{}$	Variables considered as a fixed parameter

Variables

CH	ESS charging binary decision (1 = charge)
DCH	ESS discharging binary decision (1 = discharge)
E^{ETS}	ETS thermal energy level [p.u.]
$\mathcal{I}$	Feeder current [p.u.]
$L^{ETS^{TH}}$	ETS effective thermal energy self-discharge [p.u.]
P	Active power from generating units [p.u.]
P^{ch}, P^{dch}	ESS charging, discharging power [p.u.]
P^{ETS}	ETS charging power [p.u.]
P^{LC}, Q^{LC}	Active and reactive Load curtailed [p.u.]
Q	Reactive power from generating units [p.u.]
QC	ESS reactive power output [p.u.]
S	Binary shut-down decision of generator (1 = OFF)
SOC	State of charge of ESS [p.u.]
U	Binary start-up decision of generator (1 = ON)
V	Bus voltage [p.u.]
W	ON/OFF decision (1 = ON, 0 = OFF)
δ	Voltage angle, radian

This work has been supported by NSERC Smart Microgrid Network (NSMG-NET), Canada.

B. V. Solanki, C. A. Cañizares and K. Bhattacharya are with the Department of Electrical and Computer Engineering, University of Waterloo, ON, N2L3G1, Canada (e-mail: {b2solanki, ccanizar, kankar}@uwaterloo.ca).

P. S. Sauter and S. Hohmann are with the Institute of Control Systems, Karlsruhe Institute of Technology, 76131 Karlsruhe, Germany (e-mail: {patrick.sauter, soeren.hohmann}@kit.edu).

I. Introduction

ELECTRIC Thermal Storage (ETS) systems have been used for decades for efficient use of electricity, since thermal storage allows managing charging electric power and thermal heat output separately. Thus, ETS systems store thermal energy converted from electric energy during off-peak hours and discharges as required by the thermal demand [1]. ETS systems are available for both residential and commercial applications.

Because of economic or technical reasons, there are numerous off-grid systems that are not connected to the main power grid, and thus work as isolated microgrids. In Canada, there are around 280 such isolated microgrids, most of them located in the Northern parts of the country, thus presenting significant heating demand. This high demand is generally supplied mainly by wood pallets, fuel oil, gas, and electricity [2]; however, these communities being located in remote areas, face high fuel and electricity costs compared to other parts of Canada [2]. To mitigate these cost issues and reduce environmental impact, there is a need to introduce renewable energy sources in these isolated microgrids, which requires the use of Energy Storage Systems (ESS). However, typical battery based ESS are expensive, whereas ETS is a cheaper option that can meet the thermal heating demand, and thereby allowing the efficient use of diesel- and renewable-based distributed generation (DG) units. Therefore, there is a need to properly model the ETS systems and examine their contribution in the context of microgrid Energy Management Systems (EMSs).

The potential of ETS systems for Northern electricity grids is discussed in, for example, [3] and [4]. In [3], a rule based algorithm to manage ETS charging from wind-generated electricity is presented that considers issues related with the integration of renewable energy sources and the high thermal demand in Prince Edward Island, Canada. In [4], a methodology for ETS charging, while serving as a secondary load for frequency regulation, is proposed for microgrids of Alaska, USA, with effective use of wind generation.

ETS systems as a controllable demand in the context of demand response (DR) services for single residential or commercial customers is reported in [5] and [6]. In [5], a physically based load model of ETS is presented and integrated in a load management program, the ETS is scheduled to charge only at predetermined time periods. A Model Predictive Control (MPC) based thermal storage management problem is presented in [6] for commercial buildings, considering a physical based model of thermal storage. Furthermore, various approaches to ETS system management for a cluster of residential customers, from the perspective of an aggregator, are reported in [7]–[9]. A stochastic optimization problem to schedule ETS along with a micro-combined heat and power (CHP) generator is proposed in [7] for retailers to minimize the import/export electricity and gas cost over the day; it considers the dead-band on the thermostat set-point to control the discharging of the ETS. In [8], electric space heating with partial thermal storage for a DR control strategy based on dynamic electricity pricing is presented, highlighting the benefits of DR to the aggregators. Day-ahead ETS operation strategies for an aggregator with different objectives, including electricity cost minimization, load shifting, and frequency regulation, are presented in [9], considering day-ahead hourly electricity prices. Although, the discussed works [5]–[9] present different approaches to manage ETS either for residential or commercial customers or for an aggregator, none of these have integrated the ETS into an EMS to determine the optimal schedules of DERs, including ETS systems.

The authors in [10] present an optimization based medium-term planning problem for ETS and wind resources, and a rule-based short-term operations problem for isolated microgrids in Yukon, Canada. However, the proposed short-term operations model does not consider operational constraints of fossil-fuel-based generators, grid constraints, or ESS.

In [11], a coordinated scheduling solution is presented for the introduction of combined cooling heating and power (CCHP) and ice-storage air-conditioners into grid connected microgrids with renewable generation. The system is decomposed into a stochastic day ahead scheduling and a real-time dispatching, and the optimal solution is calculated using an Improved Particle Swarm Optimization (IPSO) algorithm. The authors consider ice-storage air-conditioners, but do not consider heating ETS systems relevant to remote northern communities, and do not include constraints associated with DG units, reserve constraints, and power flow equations in neither day-ahead scheduling nor real-time dispatch.

In [12], a flexible generalized battery model (GBM) is proposed. This GBM can be used to model heating, ventilation, and air conditioning for residential and commercial buildings as well as ESS. In the GBM all the systems are modeled with the same set of parameters which makes it flexible for high-level MODELING. Also a coordination algorithm for aggregators to manage GBM is proposed to provide grid services such as frequency regulation and demand response. However, the proposed GBM model is not included in an EMS framework.

Models of ETS systems in [3] and [4] are not mathematical models, but are rather rule-based control schemes. Mathematical models in [5], [6], and [8], on the other hand, are detailed models that include thermal modeling of whole buildings, which are too complex for a real-time capable EMS. In [6] and [9], cooling ETS systems are modeled, but these have different physical characteristics. The ETS model in [7] includes CHP but like the model in [10], does not include heat losses effectively. Therefore, a simpler ETS model is proposed here, so that it can be readily integrated in a real-time EMS, considering the effective heat losses.

From the literature review, it is found that there are no works reported so far that include ETS systems in isolated microgrids with a real-time capable control based on a deterministic optimization based EMS. In addition, the EMS models proposed thus far, that the management of ETS along with other Distributed Energy Resources (DERs), do not consider detailed operating constraints associated with the DERs, network constraints, or reactive power management. There is also no study about the impact of such controlled ETS systems in the operation of northern microgirds with high penetration of renewable energy. To address the shortcomings identified in

the presented literature review, a mathematical model of ETS including heat losses is proposed in this paper for integration into a decoupled Unit Commitment (UC) and Optimal Power Flow (OPF) based EMS model, and hence determine the optimal dispatch of the DERs, along with the ETS charging control. In order to take into account the deviation in the forecast of the renewables and demand, an MPC technique is adopted in the EMS formulation. Thus, the main contributions of this work are the following:

- A new mathematical model of ETS systems is proposed considering stored thermal energy, charging electric input, thermal demand, and effective heating loss for microgrid EMS models, to analyze the impact of ETS systems on the operation of isolated microgrids.
- A novel ETS-EMS model is proposed for isolated microgrids taking into account operating UC constraints, network equations with grid constraints, deviations in the forecast of generation and demand, and the proposed ETS model.
- The ETS-EMS model is applied, tested, and validated using a modified CIGRE microgrid benchmark system and also the real Northern community's isolated microgrid of Kasabonika Lake First Nation (KLFN), Ontario, Canada, using actual measured data, demonstrating the benefits of introducing ETS systems in isolated microgrids.

The rest of the paper is organized as follows: Section II presents an overview of microgrid EMS and ETS systems. Section III discusses the mathematical model of the ETS system, the architecture of the microgrid EMS, and the mathematical models of the decoupled UC and OPF, including its MPC implementation. Section IV presents two case studies, considering the CIGRE benchmark microgrid and the KLFN microgrid, validating and demonstrating the benefits of ETS systems for the operation of isolated microgrids. Finally, Section V highlights the main conclusions and contributions of this paper.

II. Background

A. Microgrid Energy Management System

A microgrid is described as a cluster of loads, DG units, and ESS operated in coordination to reliably supply electricity, either connected to a host power system at the distribution level at a single point of connection, or in isolated from the bulk grid [13]. For the control of microgrids, as discussed in [13] and [14], the role of the EMS in microgrids is to determine the optimal commitment and dispatch of the available DERs, so that certain objectives are achieved, such as the control of the net import/export from the main grid, minimization of losses, maximization of renewables output, minimization of fossil-fuel-based generation costs, and others.

In isolated microgrids, a high level of coordination is important to balance the demand and supply while maintaining adequate reserve margins; this can be better achieved by implementing a centralized control approach [13]. Typically, a centralized microgrid EMS is based on decoupled solutions of the UC and OPF problems or considering the UC and OPF in a unified model [15]–[23]. In the UC, demand-supply balance, reserve, ESS, ramp-up and -down, minimum-up and -down time, and coordination constraints are considered with the objective to minimize the operating costs, so that optimal commitment decisions for DERs can be obtained [15]–[18]. On the other hand, the OPF minimizes the operating costs subjected to power flow, voltage, and ESS operational constraints to determine optimal active and reactive power dispatch decisions for the DERs [19], [20].

A decoupled EMS architecture comprises of 2 layers, a UC-based scheduling layer and an OPF-based dispatching layer. Both layers are solved sequentially as discussed in [21], [22] and [23]. In order to account for deviations in the forecasts of the renewables and demand, an MPC approach is used in most EMS formulations [17], [18], [21], [23]. In this work, thus, the decoupled UC and OPF based EMS is used, incorporating the ETS model proposed herein.

B. Electric Thermal Storage System

There are several kinds of ETS systems based on the storage medium, placement of the storage, and the conversion of electric energy. The storage medium can be liquid or solid. The location of the storage can be directly in the room that is heated or somewhere central to heat the whole house (e.g. in the basement). The conversion of electric energy into thermal energy can be done either by an electric heating element, i.e. a big resistance, or by a heat pump, which is more efficient but also more expensive.

In this paper, brick-core ETS systems are considered. In these systems, the conversion of the electric energy is done by heating rods that are placed between high-density bricks in which the thermal energy is stored. These bricks are in a well-insulated box to ensure low self-discharge. To discharge the heat from the thermal storage, there is a controlled fan that blows air through air channels in the bricks. The conventional ETS systems are charged during off-peak hours when electricity prices are low [24].

For different room sizes of residential buildings, there are different sizes of brick core ETS systems available, which differ in the maximum electric power and the thermal storage size. Typical systems vary in size from 1.32 to 10.8 kW and 13.5 to 40 kWh [24].

III. System Model

A. ETS Model

The schematic of house heating with ETS system is depicted in Fig. 1. The thermal demand of the house is estimated based on the ambient temperature T_a and the temperature set point T_s, using the Smart Residential Load Simulator (SRLS) [25]. As discussed in Section II.B, an ETS system comprises an electric heating element which converts the electric input $P^{ETS^{EL}}$ into thermal output $P^{ETS^{TH}}$ which is stored in high density bricks [24]. The estimated thermal demand P_s^{TH} obtained using the SRLS is considered as thermal discharge set point for the ETS. The ETS system discharges stored thermal energy to meet the thermal demand of the house, P^{TH}. In steady state, P^{TH} would be equal to P_s^{TH}; P^{TH}

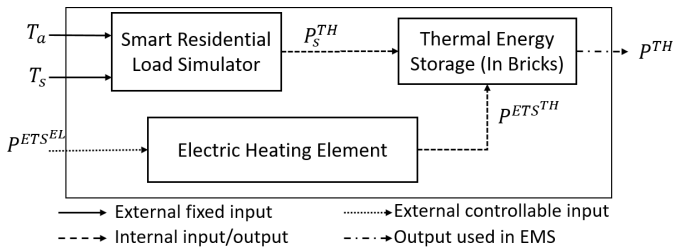

Fig. 1. Schematic of room heating with ETS system.

represents the thermal demand of typical Northern community households in the equations given next.

For the model of the ETS system, the following discrete time equations are used:

$$E_{k+1}^{ETS} = E_k^{ETS} + (P_k^{ETS^{TH}} - P_k^{TH})\Delta t_k - L_k^{ETS^{TH}} \quad \forall k \quad (1)$$

where:

$$L_k^{ETS^{TH}} \geq (1-\eta_S)E_k^{ETS}\Delta t_k - P_k^{TH}\Delta t_k \quad \forall k \in \{\mathcal{T}: (1-\eta_S)\bar{E}^{ETS} \geq \underline{P}^{TH}\} \quad (2)$$

$$L_k^{ETS^{TH}} \geq 0 \quad \forall k \in \{\mathcal{T}: (1-\eta_S)\bar{E}^{ETS} \geq \underline{P}^{TH}\} \quad (3)$$

$$L_k^{ETS^{TH}} = 0 \quad \forall k \in \{\mathcal{T}: (1-\eta_S)\bar{E}^{ETS} \leq \underline{P}^{TH}\} \quad (4)$$

Here, note that the self-discharge of the ETS is described by $(1-\eta_S)E_k^{ETS}$, while $L_k^{ETS^{TH}}$ represents the effective self-discharge of the system. As the thermal demand P^{TH} is estimated considering the room temperature to be same as temperature set point, when thermal demand is higher than the self-discharge $(1-\eta_S)E_k^{ETS}$, thermal demand P^{TH} will be same as the sum of the thermal discharge and self-discharge of the ETS. Thus, the effective self-discharge of ETS $L_k^{ETS^{TH}}$ is zero, as in (4). However, when P_k^{TH} is less than $(1-\eta_S)E_k^{ETS}$, $L_k^{ETS^{TH}}$ will be greater than zero, as given in (3) and can be calculated using (2). All other variables and parameters in these and other equations are defined in the Nomenclature section.

The conversion from electric to thermal power that is fed into the thermal energy storage can be defined as follows:

$$P_k^{ETS^{TH}} = \eta_{ETS} P_k^{ETS^{EL}} \quad \forall k \quad (5)$$

$$E_k^{ETS} \leq \bar{E}^{ETS} \quad \forall k \quad (6)$$

$$P_k^{ETS^{EL}} \leq \bar{P}^{ETS^{EL}} \quad \forall k \quad (7)$$

B. Microgrid EMS Model

The EMS problem can indeed be treated as a Mixed-Integer Non-Linear Programming (MINLP) problem, as proposed in [23], by integrating the UC and OPF models. The MINLP optimization problem was solved in [23] using the DICOPT solver, in which, first a relaxed MINLP problem was solved. Thereafter, the Non-Linear Programming (NLP) subproblems and the Mixed-Integer Programming (MIP) master problem were solved sequentially; the optimal solutions of the MIP master problem, at each iteration provided the binary decision variable which were fed into the NLP sub-problems as fixed

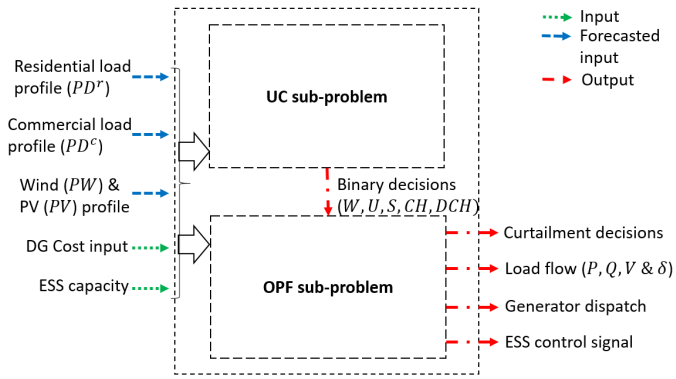

Fig. 2. EMS architecture.

decisions. However, such an MINLP problem requires long solution times not suitable for real-time applications, and may even sometimes fail to converge, as discussed in [23]. Hence, the widely used approach of decomposing the EMS problem ([21], [22] and [23]) into two subproblems, the UC and OPF, has been adopted in this work for obtaining efficient solutions suitable for real-time applications. Although, the obtained solutions are sub-optimal, they have been proven to be adequate for all practical purposes in isolated microgrid operations [13]. The microgrid EMS problem is decomposed into UC and OPF subproblems as shown in Fig. 2, and solved sequentially as discussed in [21], [22] and [23]. The UC subproblem is solved first, considering forecasted inputs from DERs to determine the commitment decisions. From the obtained solution, the binary decisions and boundary conditions are used as fixed parameters in the OPF sub-problem, which obtains the optimal dispatch of the DERs for the given forecast. The mathematical models of the UC and OPF sub-problems are explained next.

1) UC Subproblem: The objective function of this sub-problem is to minimize the operating cost of the microgrid, including generation costs, start-up and shut-down costs of diesel generators, and the significantly high costs associated with load curtailment, and can be defined as follows:

$$J = \sum_{g,k}[(a_g P_{g,k}^2 \Delta t_k + b_g P_{g,k} + c_g W_{g,k})\Delta t_k + C_g^{sup} U_{g,k} + C_g^{sdn} S_{g,k}] + \sum_{i,k}[C^{LC} P_t^{LC} \Delta t_k + x_i \mu_i C^L L_k^{ETS^{TH}}] \quad (8)$$

The model constraints are presented next:

Demand-Supply Balance: This constraint ensures that the total generation is equal to the total power demand at every time interval:

$$\sum_g P_{g,k} W_{g,k} + \sum_i (PV_{i,k} + PW_{i,k}) + \sum_n (P_{n,k}^{dch} - P_{n,k}^{ch}) = \sum_i [PD_{i,k}^r + PD_{i,k}^c + x_i \mu_i P_k^{ETS^{EL}} + x_i(1-\mu_i)P_k^{TH} - P_k^{LC}] \quad \forall k \quad (9)$$

Note that x_i represents the number of electric heating units in bus i while μ_i denotes % share of electric heating replaced by ETS at bus i.

Reserve Constraint: The following constraint guarantees that spinning reserve requirements for the microgrid are provided by the committed generators:

$$\sum_g (\bar{P}_g - P_{g,k}) W_{g,k} \geq R^{sv} \sum_i [PD^r_{i,k} + PD^c_{i,k} + x_i \mu_i P_k^{ETS^{EL}} + x_i(1-\mu_i) P_k^{TH} - P_k^{LC} + PV_{i,k} + PW_{i,k}] \quad \forall k \quad (10)$$

Generalized UC Constraints: The following constraints represent active power generation, ramp-up and ramp-down, minimum up-time and down-time limits, and coordination constraints:

$$\underline{P}_g W_{g,k} \leq P_{g,k} \leq \bar{P}_g W_{g,k} \quad \forall g,k \quad (11)$$

$$P_{g,k+1} - P_{g,k} \leq R_g^{up} \Delta t_k + U_{g,k+1} \underline{P}_g \quad \forall g, k \geq 1 \quad (12)$$

$$P_{g,k} - P_{g,k+1} \leq R_g^{dn} \Delta t_k + S_{g,k+1} \underline{P}_g \quad \forall g, k \geq 1 \quad (13)$$

$$\sum_{\hat{k}:k-T_g^{up}}^{k-1} W_{g,\hat{k}} \Delta t_{\hat{k}} > T_g^{up} S_{g,k} \quad \forall g, k > T_g^{up} \quad (14)$$

$$\sum_{\hat{k}:k-T_g^{dn}}^{k-1} (1 - W_{g,\hat{k}} \Delta t_{\hat{k}}) > T_g^{dn} U_{g,k} \quad \forall g, k > T_g^{dn} \quad (15)$$

$$U_{g,k} - S_{g,k} = W_{g,k} - W_{g,k-1} \quad \forall g, k \geq 1 \quad (16)$$

$$U_{g,k} + S_{g,k} \leq 1 \quad \forall g, k \quad (17)$$

Note that even though the DG units in microgrids have fast starting-up, shutting-down, and ramping capabilities, constraints (12)-(15) must be considered in the UC subproblem if the time resolution of the time horizon is less than the minimum start-up and shut-down times, or the time required to ramp-up/down to full capacity the respective DG units. In this work, based on [23] and [26], the minimum start-up and shut-down times of diesel generators are assumed to be 30 minutes, and full capacity ramp-up/down rates of 10 minutes are used.

Energy Storage System: The following ESS constraints include the energy balance constraint and constraints to prevent simultaneous charging/discharging, limits on State of Charge (SOC), and charging/discharging power:

$$SOC_{n,k+1} - SOC_{n,k} = \left(P_{n,k}^{ch} \eta_n^{ch} - \frac{P_{n,k}^{dch}}{\eta_n^{dch}} \right) \Delta t_k \quad \forall n, k \quad (18)$$

$$CH_{n,k} + DCH_{n,k} \leq 1 \quad \forall n, k \quad (19)$$

$$\underline{SOC}_n \leq SOC_{n,k} \leq \overline{SOC}_n \quad \forall n, k \quad (20)$$

$$P_{n,k}^{ch} \leq \overline{PESS}_n CH_{n,k} \quad \forall n, k \quad (21)$$

$$P_{n,k}^{dch} \leq \overline{PESS}_n DCH_{n,k} \quad \forall n, k \quad (22)$$

Electric Thermal Storage: The ETS constraints include the energy balance equations (1)-(5), and the limits on stored energy and charging power (6) and (7).

2) OPF Subproblem: The subproblem objective function is minimization of the operating cost of the microgrid, subject to active and reactive power balance at each node limits on active and reactive power generation of the controllable DERs, ESS constraints, and ETS constraints (1)-(7), and other grid operating constraints such as bus voltage limits. The objective function and constraints of the OPF are presented next.

Objective Function: Minimize the operating cost of the microgrid, including generation costs and costs associated with load curtailment:

$$J = \sum_{g,k} [(a_g P_{g,k}^2 \Delta t_k + b_g P_{g,k} + c_g \widehat{W}_{g,k}) \Delta t_k + C_g^{sup} \widehat{U}_{g,k} + C_g^{sdn} \widehat{S}_{g,k}] + \sum_{i,k} [C^{LC} P_t^{LC} \Delta t_k + x_i \mu_i C^L L_k^{ETS^{TH}}] \quad (23)$$

Power Balance: The power balance equation at each bus considers the output from DG, PV and wind units, and the total power demand of loads from commercial and residential customers, taking into account ESS charging and discharging:

$$\sum_{g \in G_i} P_{g,k} + PV_{i,k} + PW_{i,k} + x_i \mu_i P_k^{ETS_{EL}} + x_i(1-\mu_i) P_k^{TH} - PD^c_{i,k} V_{i,k}^{\alpha_k^c} - [PD^r_{i,k} - P_k^{LC}] V_{i,k}^{\alpha_k^r} + \sum_{n \in N_i} (P_{n,k}^{dch} - P_{n,k}^{ch}) = \sum_j V_{i,k} V_{j,k} Y_{i,j} \cos(\theta_{i,j} + \delta_{j,k} - \delta_{i,k}), \forall k, i, j \quad (24)$$

$$\sum_{g \in G_i} Q_{g,k} - QD^c_{i,k} V_{i,k}^{\beta_k^c} - (QD^r_{i,k} - Q_k^{LC}) V_{i,k}^{\beta_k^r} + \sum_{n \in N_i} (QC_{n,k}) = -\sum_j V_{i,k} V_{j,k} Y_{i,j} \sin(\theta_{i,j} + \delta_{j,k} - \delta_{i,k}), \forall k, i, j \quad (25)$$

Here, residential and commercial loads are modeled as exponential functions of voltage.

Reserve Constraint: Even though the commitment decisions of DERs are obtained from the UC subproblem considering spinning reserves, reserve constraints still need be included in the OPF subproblem to ensure proper operating margins. Thus, equation (10) is modified in the OPF as follows:

$$\sum_g (\bar{P}_g - P_{g,k}) \widehat{W}_{g,k} \geq R^{sv} \sum_i [PV_{i,k} + PW_{i,k} + PD^c_{i,k} V_{i,k}^{\alpha_k^c} + x_i \mu_i P_k^{ETS} + x_i(1-\mu_i) P_k^{TH} + (PD^r_{i,k} - P_k^{LC}) V_{i,k}^{\alpha_k^r}], \forall k \quad (26)$$

Note that $\widehat{W}_{g,k}$ in (26) are the optimal UC decisions which are applied in the OPF as fixed parameters.

Grid Operational Constraints: These include (11)-(13) with the binary variables $W_{g,k}, U_{g,k}$ and $S_{g,k}$ now being known parameters and also the following equations:

$$\underline{Q}_g \widehat{W}_{g,k} \leq Q_{g,k} \leq \bar{Q}_g \widehat{W}_{g,k} \quad \forall g, k \quad (27)$$

$$\underline{V} \leq V_{i,k} \leq \bar{V} \quad \forall k \quad (28)$$

$$\mathcal{I}_{i,j,k_t}(|V_{i,k_t}|, |V_{j,k_t}|, |\delta_{i,k_t}|, |\delta_{j,k_t}|) \leq \overline{\mathcal{I}}_{i,j} \quad \forall i, j, k_t \quad (29)$$

where these constraints impose limits on the reactive power generation and voltage at each node, and feeder current limits.

Energy Storage System: The ESS constraints include (18)

and (20), while (19), (21), and (22) are replaced by the following equations:

$$P^{ch}_{n,k} P^{dch}_{n,k} = 0 \qquad \forall n, k \qquad (30)$$

$$P^{ch}_{n,k} \leq \overline{PESS}_n \qquad \forall n, k \qquad (31)$$

$$P^{dch}_{n,k} \leq \overline{PESS}_n \qquad \forall n, k \qquad (32)$$

3) Implementation: As discussed in [21], [22] and [23], in the decomposition approach, UC and OPF subproblems are solved sequentially. The UC subproblem corresponding to a Mixed Integer Quadratic Programming (MIQP) problem is solved first. From the obtained feasible UC solution, the binary UC decisions and boundary conditions are used as fixed parameters to solve the OPF subproblem. The OPF subproblem is a Non-Linear Programming (NLP) problem and the obtained OPF solution will be the dispatch for the DERs.

4) Model Predictive Control: In order to capture the deviations in forecasts of renewables and demand, an MPC approach is used, in which the optimization problem is solved at discrete time steps considering updated forecast inputs on a rolling time horizon, with the obtained optimal solution being valid only for the next time step [17], [18], [21], [23], [27]. The proposed EMS approach is decomposed into two subproblems, a UC problem and an OPF problem, the UC being an MIQP problem while the OPF is an NLP problem; and accordingly the MPC intervals and horizons of the two subproblems are different. Hence, there are two MPC problems which are being solved sequentially, both based on iterative, finite-horizon optimization of a system model. Thus, from the obtained UC and OPF solutions for the time horizon $\tau_k = \{k, \ldots, k+T\}$, only the solution for the current time step k is used, and at time $k+1$, the forecasts are updated for a shifted time horizon $\tau_{k+1} = \{k+1, \ldots, k+1+T\}$; the whole process is repeated every time interval. In this work, a recalculation time of 5 minutes is used in the implementation of the MPC approach.

The time horizon is important for an MPC-based EMS, since the longer the time horizon, the better is the solution obtained [17]; however, this adds to the computational burden of the EMS. A reasonable time horizon for the UC subproblem is 24 hours [21]. On the other hand, since the forecasting error increases with the increase in forecast lead time, non-uniform 24 hour MPC control and prediction time intervals are considered for the UC subproblem; thus, the first 12 time intervals are of 5 minutes, the next 6 time intervals are of 15 minutes, the following 5 time intervals are of 30 minutes, and the final 19 time intervals are 1-hour long [21], [23]. For the OPF sub-problem, the control intervals are of 5 minutes for a 1 hour horizon. The MPC time intervals and horizons for both UC and OPF problems are depicted in Fig. 3.

IV. Results

The EMS model is coded in GAMS [28], the UC sub-problem is a mixed integer quadratic programming (MIQP) problem (linear constraints, with a quadratic objective function) solved using the CPLEX solver [29], in which the maximum absolute relative gap is set at 1%, which corresponds to a maximum difference of 1% between the best possible integer solution and the global optimal non-integer solution. The OPF sub-problem is a Non-Linear Programming (NLP) problem, solved using the SNOPT solver. This approach provides a locally optimal solution, which may or may not be the global optimal solution. However, as discussed in [13], sub-optimal solutions for EMS models are adequate for practical purposes in microgrid operation.

TABLE I
DER ratings for modified CIGRE system [23].

Node	DER type	Pmax [kW]
1	Diesel Generator	800
9	CHP diesel	310
1	Diesel Generator	1400
1	Diesel Generator	2500
3	Photovoltaic	600
4	Photovoltaic	33
5	Photovoltaic	30
5	Battery	750
5	Residential fuel cell	41.25
6	Photovoltaic	50
8	Photovoltaic	200
9	Photovoltaic	212
9	Fuel cell	265
10	Photovoltaic	214
10	Battery	250
10	Residential fuel cell	17.5
13	CHP Microturbine	500
7	Wind turbine (inverter-interfaced)	1000
7	Wind turbine (SCIG)	500

The developed ETS-EMS model is tested and validated on an isolated microgrid corresponding to a modified CIGRE benchmark system [21], with further modifications discussed in [23]. The proposed approach is then applied to real Northern Communities' isolated microgrid of KLFN, Ontario, Canada to evaluate its practical application and possible benefits. The MPC based ETS-EMS framework is simulated on both systems for 6 days, from 25 to 30 January, 2015, considering the same ambient temperature profile for both test systems (KLFN data from [30] was used). The demand, wind, and solar profiles for the KLFN system are real measured data, while for the modified CIGRE test system these data are provided in [21] for a single day which are perturbed considering normal probability density functions (p.d.f.s) to simulate different days. To simulate forecast errors, normal p.d.f.s were used to perturb the actual profiles, as discussed in [23]. The ETS system self-discharge rate $(1 - \eta_S)$ used for these studies is 0.2 %/h [10].

A. CIGRE Benchmark System

The modified CIGRE benchmark system with 25% more ESS capacity, shown in Fig. 12, and in Table I is used to test and validate the developed ETS-EMS framework; the total installed capacity is 9,216 kW including all DERs, considering feeder current limits [23]. For the presented studies, 50% of the total residential demand is assumed to be electric heating demand [31]. The electric heating demand profile is obtained by using the Smart Residential Load Simulator [25], considering typical parameters of detached single houses in Canada [32].

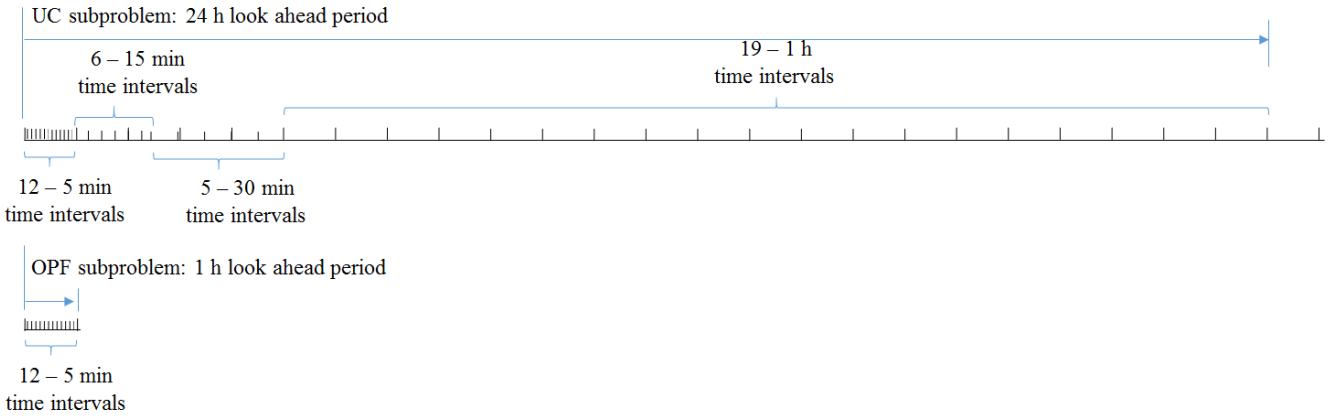

Fig. 3. Time horizon.

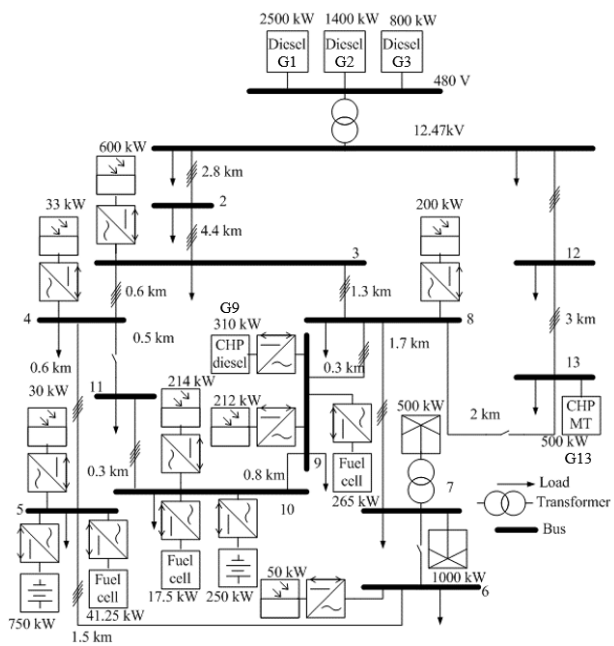

Fig. 4. Modified CIGRE benchmark system [23].

TABLE II
SUMMARY OF RESULTS FOR CIGRE SYSTEM

Case	Operating Cost of Microgrid	Peak Demand	Energy Curtailed	Dispatch Share [%]	
	[$]	[MW]	[kWh]	ESS	G3
I	148,718	6.76	293	1.4	4
II	117,136	6.43	0	0.5	2.6
III	116,735	6.47	0	0.34	1.9

Three cases are analyzed:

- Case I: No ETS system.
- Case II: 50% of the electric heating demand is provided by ETS.
- Case III: 100% of the electric heating demand is provided by ETS.

Table II presents a summary of the results for all cases for the modified CIGRE benchmark system. Observe that there is a significant difference in the operating cost of microgrid between Case I and the other two cases, where electric heating is provided by the ETS system, because of the load curtailment required in Case I. Thus, with the introduction of ETS systems, the peak demand is reduced by 4.9% and 4.3% in Cases II and III, respectively. It is also noted that the share of energy supplied by the ESS and the most expensive generator (G3) in the total energy dispatch, is reduced significantly from Case I to Case III, which further reduces the operating costs, and demonstrates the diminishing role of ESS when ETS is introduced. It should be mentioned that for this practical system [33], the feeder current limits were enforced but did not become active, which is consistent with what has been observed in real microgrids, where the feeder capacity is designed to be greater than the maximum system demand, as in case of the Huatacando microgrid in Chile [17], the Bella Coola microgrid [34], and Hartley Bay microgrid in British Columbia, Canada [35], and therefore feeder limits have not been considered in the EMS models of these microgrids.

Figure 5 presents a stacked-area plots of the optimal dispatch for the first day obtained for all the cases considered. The negative areas in these plots correspond to the charging of the ESS, and the dark grey line depicts the total demand including electric heating. The black dotted line denotes the total demand including the electric heating load and including the ETS charging power. Finally, the white area below the demand line corresponds to load curtailment. Observe in these plots the following:

- In Case I, load curtailment during hours 9 and 10 takes place due to insufficient generation capacity.
- In Case II, a significant reduction in use of ESS can be observed due to the introduction of the ETS systems. In Case III, the use of ESS is almost negligible.
- With the introduction of ETS system, the use of the most expensive generator G3 is reduced. While in Case I, the share of G3 in the dispatch is 4%, which is reduced to 2.6% in Case II and further reduced to 1.9% in Case III.

Figure 6 depicts the ETS charging power, the ETS energy levels, and the thermal demand for Case III. Note that in the time Windows 1 and 5, the ETS is charged during the off-peak hours, while in on-peak hours in Windows 2 and 4,

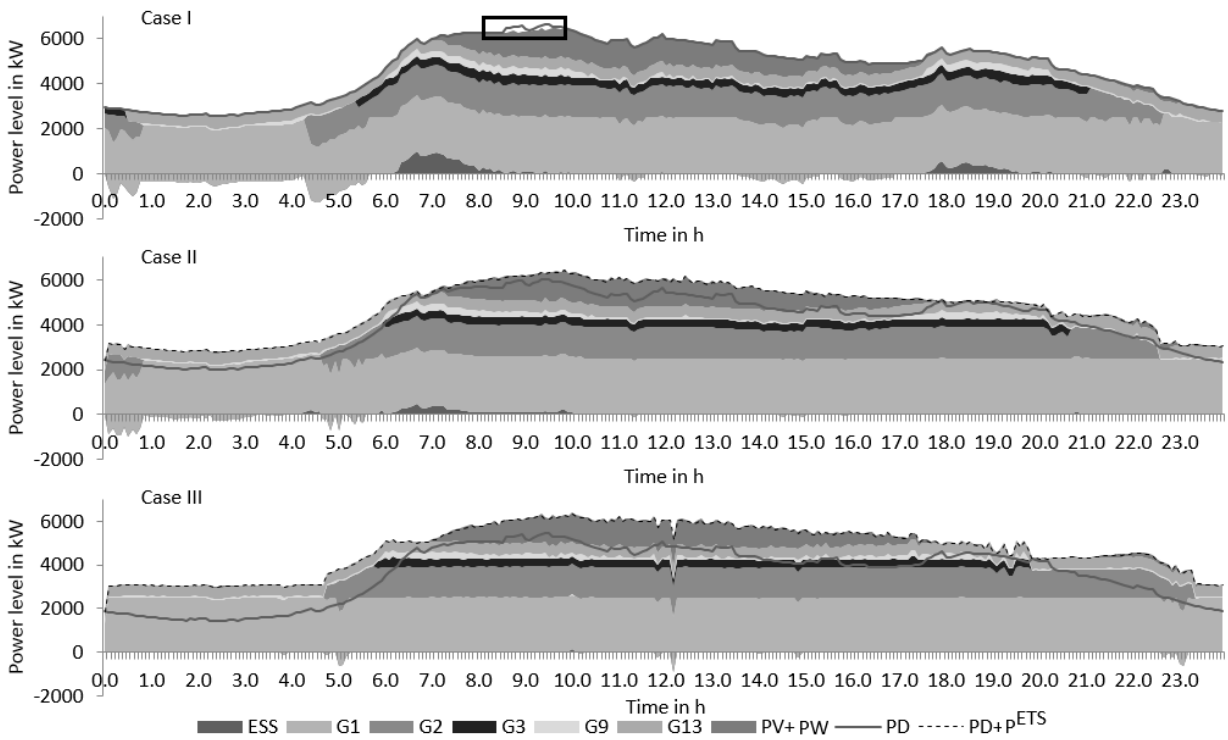

Fig. 5. Dispatch for all three cases for the CIGRE test system.

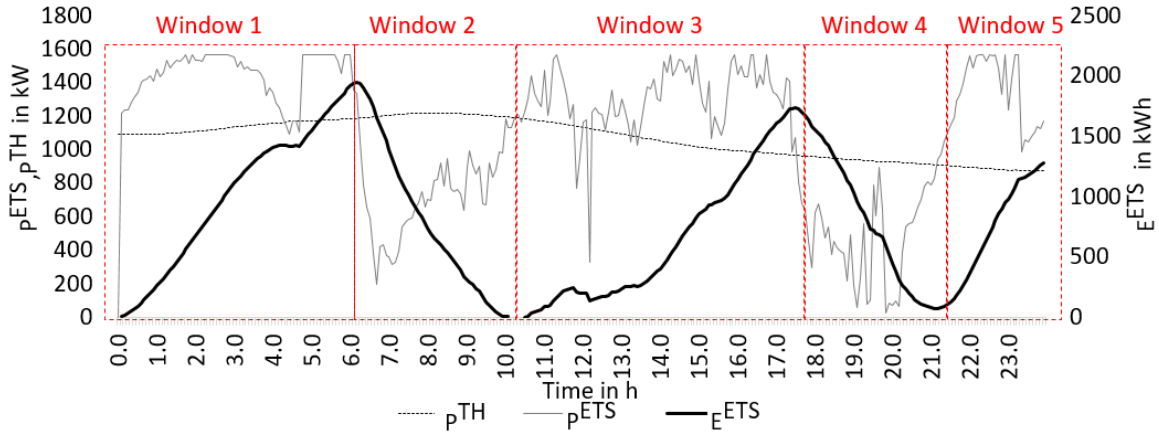

Fig. 6. ETS charging power and energy, and thermal demand for the CIGRE test system.

the ETS is not charged, using the stored energy to meet the thermal demand. In Window 3, when energy from renewables is available, the ETS is charged again. This matches the dispatch and use of ETS discussed in [10].

B. Kasabonika Lake First Nation System

The KLFN system model used in this paper, shown in Fig. 7 with generator cost data given in Table III, allows to evaluate the potential contribution of ETS systems in a real existing Northern community microgrid. As the KLFN community is planning to build a new 250 kW PV plant, the system is analyzed with and without this solar plant, considering feeder current limits.

The measured PV generation data of existing 12.4 kW rooftop PV panels is used in all simulations. Measured data for the existing wind turbines is also used. There are 3 diesel units operated one a time, with a maximum installed capacity of 1.5 MW. The commercial demand is represented by the measured data from the store (SRT), the school (SCL), the police station (PLC), the nursery station (NRS), and the water treatment plant (WTP). The total residential demand profile

TABLE III
GENERATOR COST DATA FOR KLFN SYSTEM

DG unit	a	b	c	C^{sup}	C^{sdn}
G1	0.000123	1.0027	107.3	83.6	13.464
G2	0	0.5	88.06	39.6	7.304
G3	1.87E-05	0.1712	37.69375	13.2	4.664

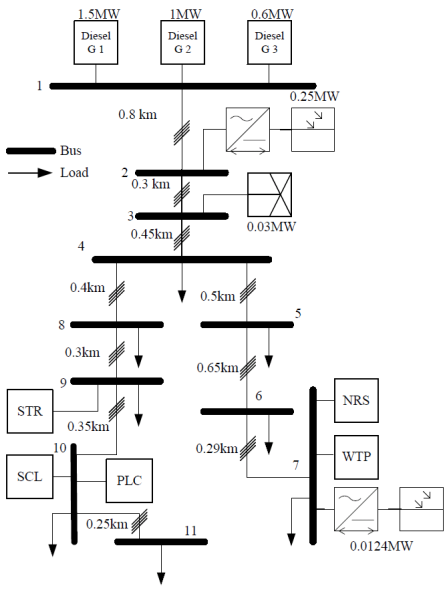

Fig. 7. Kasabonika Lake First Nation system.

TABLE IV
SUMMARY OF RESULTS FOR KLFN SYSTEM

250 kW PV Plant	Case	Operating Cost of Microgrid, [$]	Peak Demand, [kW]	Total ON Time [h] G2	Total ON Time [h] G3
No	I	45,724	771	97	47
	II	43,574	734	89	55
	III	40,220	790	73	71
Yes	I	42,632	771	90	54
	II	36,710	725	65	79
	III	32,898	772	49	95

is calculated from the measured total generation net of the total commercial demand profiles, assuming that losses are not really significant in this microgird, given the length of the feeders.

In this system, 30% of the total residential electricity demand is assumed to be from electric heating demand [36]. The electric heating demand profile is obtained in this work using the Smart Residential Load Simulator [25], considering parameters of a typical KLFN house and measured ambient temperature data [30].

As in the CIGRE system, three cases are analyzed:

- Case I: No ETS system.
- Case II: 50% of the electric heating demand replaced by ETS.
- Case III: 100% of the electric heating demand replaced by ETS.

Table IV shows the results for all these cases, with and without the 250 kW PV plant. Note the significant reduction in operating costs by increasing the penetration of ETS in both scenarios; without the PV plant, the maximum cost reduction is 12%, and with the PV plant, a cost reduction of up to 22.8% is possible. Observe that the peak demand is not reduced in this system; which however, is only around 50% of the maximum capacity of the system. As with the

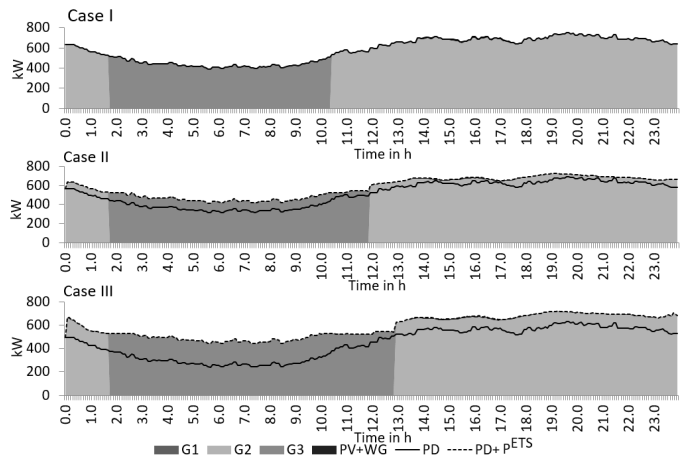

Fig. 8. Dispatch for all cases for the KLFN system without 250 kW PV plant.

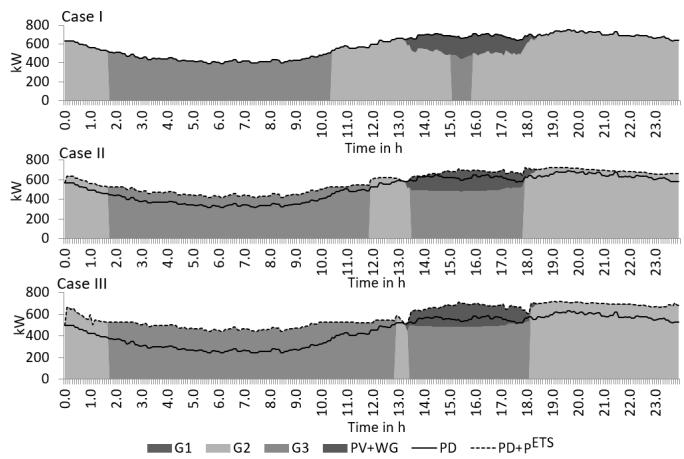

Fig. 9. Dispatch for all cases for the KLFN system with 250 kW PV plant.

modified CIGRE benchmark system, feeder current limits were not reached, given that the feeder capacities are typically designed to be larger than the system peak demand in such real microgrids [17], [33]–[35].

In Figs. 8 and 9, the stacked-area plots of the optimal dispatch obtained for all the cases and both scenarios of PV plant are depicted for the first day. The following observations can be made:

- The demand can be met by one of the two smaller generators at all times, since in the considered days, the demand was not high enough to dispatch the new 1.5 MW generator, G1.
- With the increase of ETS penetration, the total time G3 is ON increases (see Table IV) which highlights efficient operation of generators since G3 operates near its maximum capacity with increased ON time so that total ON time of G2 which operates at low efficient operating point due to low demand compared to its capacity, is decreased.
- Because of inclusion of ETS when system has no significant penetration of renewable power, generators G2 and G3 operate about the same amount of time, near their

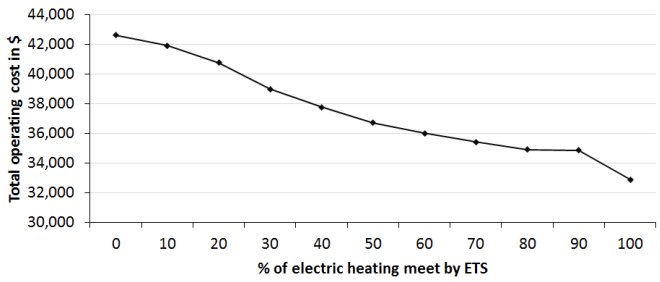

Fig. 10. Percentage of electric heating replaced by ETS systems versus operating costs.

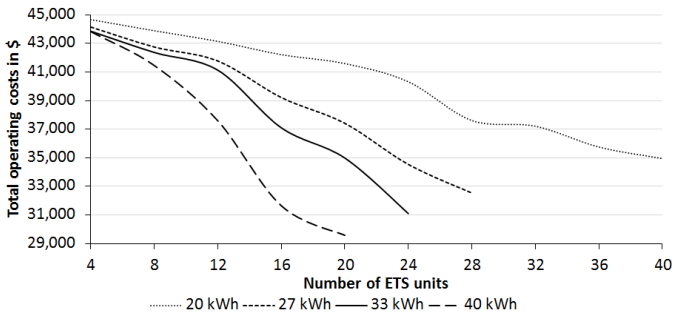

Fig. 11. Variation of total operating cost with number of ETS units.

optimal operating point. As the PV power penetration is increased, the smaller generator is used more, as expected [36].

To analyze the reduction of cost with respect to ETS penetration, the share of ETS is increased from 0% to 100% in steps of 10% in the scenario with the 250 kW PV plant. The impact of this increase on the operating costs is shown in Fig. 10; where it can be observed that the operating cost steadily decreases as the ETS penetration increases. These results support the introduction of ETS systems in the KLFN community.

C. Sensitivity Study

In order to analyze the impact of the location, capacity and the number of ETS units on operating costs, a sensitivity study is presented, considering the KLFN isolated microgrid, using actual measured electricity demand, and output from PV and wind generators. The 6-day dispatch problem was repeated considering various commercially available ETS unit capacities of 20 kWh, 27 kWh, 33 kWh, and 40 kWh [24], and varying the number of ETS units from 4 to 40, depending on the ETS capacity. Fig. 11 shows that the total operating cost reduces with the number of ETS units in a linear manner for all ETS capacities. Also note that the overall 6-day least operating cost is obtained with 20 units of 40 kWh ETS, while for the other ETS unit capacities, the minimum operating cost increases with decrease in the ETS capacity.

Figure 12 shows the variation of total operating cost with total ETS capacity for different ETS unit capacities considered. Observe that the 40 kWh ETS is the cheapest option in most cases due to its larger charging power limits, as compared to all other ETS unit capacities.

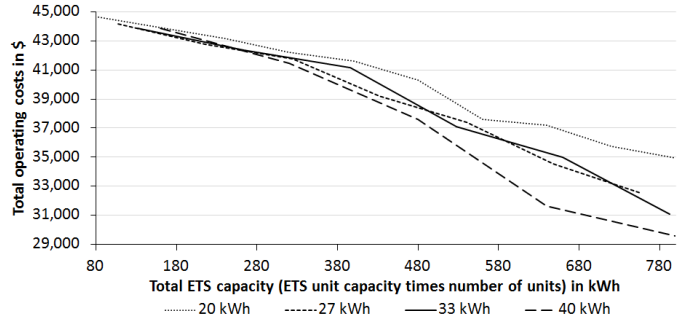

Fig. 12. Variation of total operating cost with total ETS capacity.

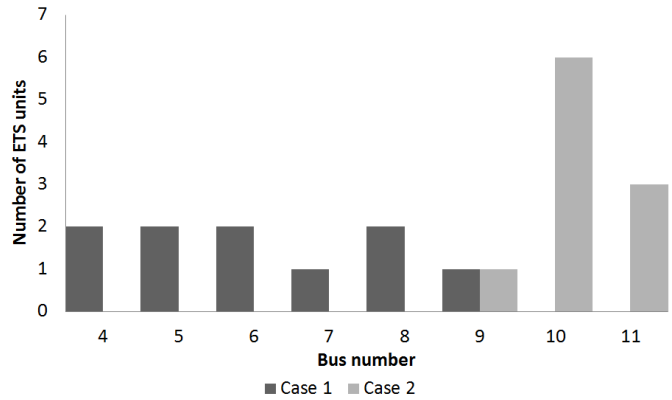

Fig. 13. Distribution of number of ETS units at various buses.

To analyze the impact of the location of ETS systems, the 6-day dispatch problem was solved assuming that 50% of the households with electric heating have a 40 kWh ETS, and changing the number of houses per bus with ETS. As shown in Fig. 13, two ETS distributions per bus are considered, in Case 1, the ETS are located at Buses 4-9 only, which are closer to the generators; while in Case 2, the ETS are located at Buses 9-11, which are farthest from the generators. As expected, because of the typical size of the KLFN isolated microgrid, the operating costs obtained for the two cases are more or less the same, indicating that the location of ETS systems do not significantly impact the operating costs of the considered microgrid.

V. Conclusions

A mathematical model for an ETS system was presented and integrated into a decoupled UC-OPF microgrid EMS model, with an MPC approach to account for the deviations in the forecast of renewables and demand. The proposed ETS-EMS framework was tested and validated using a modified CIGRE benchmark system, highlighting the benefits of integration of ETS systems in terms of reduction in operating costs, load curtailment, and use of ESS. Additionally, the ETS-EMS model was applied to the KLFN isolated microgrid, showing a possible reduction in operating costs of up to 23%, showing that the higher the penetration of renewables, the more reduction in operating costs, with diesel units operating closer to their optimal point. A sensitivity study was also performed to analyze the impacts of the location, number,

and unit capacity of the ETS systems on the operating costs of KLFN microgrid system, illustrating that the location has negligible impact on operating costs, while the operating costs decrease linearly with the number of ETS units, and as the capacity of the ETS units increase, the operating cost decreases.

REFERENCES

[1] W. R. Coleman and C. M. Grastataro, "American electric power system electric thermal storage program: An evaluation of performance within the home," *IEEE Trans. Power App. Syst.*, vol. PAS-100, no. 12, pp. 4741–4749, Dec. 1981.

[2] M. Arriaga, C. A. Cañizares, and M. Kazerani, "Northen Lights: Access to electricty in Canada's northern and remote communities," *IEEE Power Energy Mag.*, vol. 12, no. 4, pp. 50–59, Jul/Aug 2014.

[3] L. Hughes, "Meeting residential space heating demand with wind-generated electricity," *Ren. Energy*, vol. 35, pp. 1765–1772, 2010.

[4] N. T. Janssen, R. A. Peterson, and R. W. Wies, "Improved frequency regulation on hybrid wind-diesel microgrids using self-sensing electric thermal storage devices," in *Proc. IEEE Australasian Universities Power Engineering Conference (AUPEC),* Curtin University, Perth, Australia, Sep.-Oct. 2014, pp. 1–6.

[5] A. Molina, A. Gabaldonó, C. Álvarez, J. A. Fuentes, and E. Gómez, "A physically based load model of residential electric thermal storage: Application to LM programs," *Int. J. Energy Res.*, vol. 24, no. 1, pp. 1–6, 2004.

[6] K. J. Kircher and K. M. Zhang, "Model predictive control of thermal storage for demand response," in *Proc. IEEE American Control Conference,* Chicago, IL, USA, 2015, pp. 956–961.

[7] N. Good, E. Karangelos, A. Navarro-Espinosa, and P. Mancarella, "Optimization under uncertainty of thermal storage-based flexible demand response with quantification of residential users' discomfort," *IEEE Trans. Smart Grid*, vol. 6, no. 5, pp. 2333–2342, Sep. 2015.

[8] M. Ali, J. Jokisalo, K. Siren, and M. Lehtonen, "Combining the demand response of direct electric space heating and partial thermal storage using LP optimization," *Elect. Power Syst. Res.*, vol. 106, pp. 160–167, Jan. 2014.

[9] Y. Tang and J. Zhong, "Operation strategies and performance of air-conditioning systems with thermal energy storages in power systems," in *Proc. IEEE Power Systems Computation Conference (PSCC),* Genova, Italy, Jun. 2016.

[10] S. Wong and J. Pinard, "Opportunities for smart electric thermal storage on electric grids with renewable energy," *IEEE Trans. Smart Grid,* pre-print, pp. 1–9, Jan. 2016.

[11] Z. Bao, Q. Zhou, Z. Yang, Q. Yang, L. Xu, and T. Wu, "A multi time-scale and multi energy-type coordinated microgrid scheduling solution-part i: Model and methodology," *IEEE Trans. Power System*, vol. 30, no. 5, pp. 2257–2266, Nov. 2014.

[12] H. Hao, D. Wu, J. Lian, and T. Yang, "Optimal coordination of building loads and energy storage for power grid and end user services," *IEEE Trans. Smart Grid,* pre-print, pp. 1–11, Jan. 2017.

[13] IEEE-PES Task Force on Microgrid Control, "Trends in microgrid control," *IEEE Trans. Smart Grid*, vol. 5, no. 4, pp. 1905–1919, Jul. 2014.

[14] F. Katiraei, R. Iravani, N. Hatziargyriou, and A. Dimeas, "Microgrids management: Controls and operation aspects of microgrids," *IEEE Power Energy Mag.*, vol. 6, no. 3, pp. 54–65, May/Jun 2008.

[15] H. Kanchev, F. Colas, C. Lazarov, and B. Francois, "Emission reduction and economical optimization of an urban microgrid operation including dispatched PV-based active generators," *IEEE Trans. Sustainable Energy*, vol. 5, no. 4, pp. 1397–1405, Oct. 2014.

[16] C. Chen, S. Duan, T. Cai, B. Liu, and G. Hu, "Smart energy management system for optimal microgrid economic operation," *IET Renewable Power Generation*, vol. 5, no. 3, pp. 258–267, 2011.

[17] R. Palma-Behnke, C. Benavides, F. Lanas, B. Severino, L. Reyes, J. Llanos, and D. Saez, "A microgrid energy management system based on the rolling horizon strategy," *IEEE Trans. Smart Grid*, vol. 4, no. 2, pp. 996–1006, Jun. 2013.

[18] A. Parisio, E. Rikos, and L. Glielmo, "A model predictive control approach to microgrid operation optimization," *IEEE Trans. Control Syst. Technol.*, vol. 22, no. 5, pp. 1813–1827, Sep. 2014.

[19] S. Y. Derakhshandeh, A. S. Masoum, S. Deilami, M. A. S. Masoum, and M. E. H. Golshan, "Coordination of generation scheduling with PEVs charging in industrial microgrids," *IEEE Trans. Power Syst.*, vol. 28, no. 1, pp. 102–111, Feb. 2013.

[20] S. Conti, R. Nicolosi, S. A. Rizzo, and H. H. Zeineldin, "Optimal dispatching of distributed generators and storage systems for MV islanded microgrids," *IEEE Trans. Power Delivery*, vol. 27, no. 3, pp. 1243–1251, May 2012.

[21] D. E. Olivares, C. A. Cañizares, and M. Kazerani, "A centralized energy management system for isolated microgrids," *IEEE Trans. Smart Grid*, vol. 5, no. 4, pp. 1864–1875, Jul. 2014.

[22] Q. Jiang, M. Xue, and G. Geng, "Energy management of microgrid in grid-connected and stand-alone modes," *IEEE Trans. Power System*, vol. 28, no. 3, pp. 3380–3389, Aug. 2013.

[23] B. V. Solanki, A. Raghurajan, K. Bhattacharya, and C. A. Cañizares, "Including smart loads for optimal demand response in integrated energy management systems for isolated microgrids," *IEEE Trans. Smart Grid,* pre-print, pp. 1–10, Dec. 2015.

[24] STEFFES ETS room unit specifications. [Online]. Available: http://www.steffes.com/electric-thermal-storage/room-units/

[25] E. Pouresmaeil, J. M. Gonzalez, C. A. Cañizares, and K. Bhattacharya, "Development of a smart residential load simulator for energy management in smart grids," University of Waterloo, Waterloo, Canada, Tech. Rep. [Online]. Available: https://uwaterloo.ca/power-energy-systems-group/sites/ca.power-energy-systems-group/files/uploads/files/srls.pdf

[26] P. Marty, "Design of a hybrid power pv genset battery storage system for a remote off-grid application in malaysia," Master's thesis, KTH School of Industrial Engineering and Management, Stockholm, Sweden, 2016.

[27] R. Findeisen, "Nonlinear model predictive control: A sampled-data feedback perspective," Ph.D. dissertation, Univ. Stuttgart, Stuttgart, Germany, 2004.

[28] R. E. Rosenthal, "GAMS - A user's guide," Tech. Rep., May 2015. [Online]. Available: http://www.gams.com/dd/docs/bigdocs/GAMSUsersGuide.pdf

[29] "GAMS - The solver manuals," Tech. Rep., May 2015. [Online]. Available: http://www.gams.com/dd/docs/solvers/allsolvers.pdf

[30] Weather historical data. [Online]. Available: http://climate.weather.gc.ca/historical˙data/search˙historic˙data˙e.html

[31] Household consumption. [Online]. Available: http://www.hydroquebec.com/residential/energy-wise/why/electricity-consumption-by-use.html

[32] "Households and the environment: Energy use," Statistics Canada - Environment Accounts and Statistics Division, Tech. Rep., 2011. [Online]. Available: http://www.statcan.gc.ca/pub/11-526-s/11-526-s2013002-eng.pdf

[33] K. Rudion, A. Orths, Z. Styczynski, and K. Strunz, "Design of benchmark of medium voltage distribution network for investigation of DG integration," in *Proc. IEEE PES Gen. Meet.*, Jun. 2006.

[34] A. Hajimiragha and M. R. D. Zadeh, "Research and development of a microgrid control and monitoring system for remote community of Bella Coola: Challenges, solutions, achievements and lessons learned," in *Proc. IEEE Int. Conf. on Smart Energy Grid Eng. (SEGE)*, Aug. 2001.

[35] "The first canadian smart remote microgrid: Hartley Bay, BC," Natural Resources Canada, Tech. Rep. [Online]. Available: http://www.nrcan.gc.ca/sites/www.nrcan.gc.ca/files/canmetenergy/files/pubs/2013-035˙en.pdf

[36] M. Arriaga, "Long-term renewable energy electricity planning for remote communities," Ph.D. dissertation, University of Waterloo, Waterloo, Ontario, Canada, 2015.

Patrick S. Sauter studied electrical engineering and information technologies at Karlsruhe Institute of Technology (KIT), Karlsruhe, Germany, where he received the B. Sc. degree in 2010 and M. Sc. degree in 2013. He is a research assistant with the Institute of Control Systems at KIT, where he is currently pursuing the Ph.D. degree. His current research interests include modelling and optimal control of distribution grids and multi-carrier energy systems.

Bharatkumar V Solanki (S'14) received the Bachelor's degree in electrical engineering from Gujarat University, Ahmedabad, India in 2009, and the Master's degree in Electrical Engineering from the Maharaja Sayajirao University of Baroda, Vadodara, India in 2011. He worked as an analog hardware design engineer in ABB Global Industries and Service Limited, India from 2011 to 2013. He is currently working toward his Ph.D. degree in Electrical and Computer Engineering at the University of Waterloo, Waterloo, ON, Canada. His research interests include modeling, simulation, control and optimization of power systems.

Claudio A. Cañizares (S'85,M'91,SM'00,F'07) is a Full Professor and the Hydro One Endowed Chair at the Electrical and Computer Engineering (E&CE) Department of the University of Waterloo, where he has held various academic and administrative positions since 1993. He received the Electrical Engineer degree from the Escuela Politècnica Nacional (EPN) in Quito-Ecuador in 1984, where he held different teaching and administrative positions between 1983 and 1993, and his MSc (1988) and PhD (1991) degrees in Electrical Engineering are from the University of Wisconsin-Madison. His research activities focus on the study of stability, modeling, simulation, control, optimization, and computational issues in large and small girds and energy systems in the context of competitive energy markets and smart grids. In these areas, he has led or been an integral part of many grants and contracts from government agencies and companies, and has collaborated with industry and university researchers in Canada and abroad, supervising/co-supervising many research fellows and graduate students. He has authored/co-authored a large number of journal and conference papers, as well as various technical reports, book chapters, disclosures and patents, and has been invited to make multiple keynote speeches, seminars, and presentations at many institutions and conferences world-wide. He is an IEEE Fellow, as well as a Fellow of the Royal Society of Canada, where he is currently the Director of the Applied Science and Engineering Division of the Academy of Science, and a Fellow of the Canadian Academy of Engineering. He is also the recipient of the 2017 IEEE Power & Energy Society (PES) Outstanding Power Engineering Educator Award, the 2016 IEEE Canada Electric Power Medal, and of various IEEE PES Technical Council and Committee awards and recognitions, holding leadership positions in several IEEE-PES Technical Committees, Working Groups and Task Forces.

Kankar Bhattacharya (M'95,SM'01,F'17) received the Ph.D. degree in electrical engineering from the Indian Institute of Technology, New Delhi, India, in 1993. He was with the Faculty of Indira Gandhi Institute of Development Research, Mumbai, India, from 1993 to 1998, and with the Department of Electric Power Engineering, Chalmers University of Technology, Gothenburg, Sweden, from 1998 to 2002. In 2003, he joined the Electrical and Computer Engineering Department, University of Waterloo, Waterloo, ON, Canada, where he is currently a full Professor. His current research interests include power system economics and operational aspects. He is a Registered Professional Engineer in the province of Ontario.

Sören Hohmann studied electrical engineering at the Technische Universit´at Braunschweig, University of Karlsruhe and école nationale supérieure d'électricité et de mécanique Nancy. He received the diploma degree (1997) and Ph.D. degree (2002) from University of Karlsruhe. Afterwards, until 2010 he worked in the industry for BMW, Munich, where his last position was head of the predevelopement and series developement of active safety systems. Today he is the head of the Institute of Control Systems at the Karlsruhe Institute of Technology, Germany as well as a directors board member of the research center for information technology (FZI), Karlsruhe. His research interests are cooperative control, alternative energies and system guarantees by design.